

TOPICAL REVIEW • **OPEN ACCESS**

Emerging concept of photocatalytic lung assist device - a review

To cite this article: A Subrahmanyam *et al* 2020 *J. Phys. Mater.* **3** 032003

View the [article online](#) for updates and enhancements.



ECS The Electrochemical Society
Advancing solid state & electrochemical science & technology
2021 Virtual Education

Intensive Short Courses

Sun, Oct 10 & Mon, Oct 11

Providing students and professionals with in-depth education on a wide range of topics

Early registration deadline: Sep 13, 2021

Register early and save!

The advertisement features a woman with curly hair wearing a headset and smiling while working on a laptop at a desk. The background shows a corkboard with various notes and a small potted plant on the desk.



TOPICAL REVIEW

Emerging concept of photocatalytic lung assist device - a review

OPEN ACCESS

RECEIVED
6 January 2020REVISED
16 May 2020ACCEPTED FOR PUBLICATION
27 May 2020PUBLISHED
30 June 2020A Subrahmanyam¹ , Deepak Kumar Kaushik² and T Paul Ramesh³¹ Department of Physics, Indian Institute of Technology Madras, Chennai 600036, India² Department of Physics, Lovely Professional University, Phagwara, India³ Department of Cardiothoracic Surgery, Apollo Hospital, Greams Road, Chennai, IndiaE-mail: manu@iitm.ac.in and manuiitm2014@gmail.com**Keywords:** lung assist device, photocatalysis, oxygenation of blood, titanium oxide and indium tin oxide thin films, photo Hall effect

Original content from this work may be used under the terms of the [Creative Commons Attribution 4.0 licence](https://creativecommons.org/licenses/by/4.0/).

Any further distribution of this work must maintain attribution to the author(s) and the title of the work, journal citation and DOI.

**Abstract**

The increasing incidence of lung disease and progress to end stage respiratory failure has focused attention on the need for lung assist devices. Hollow fibre membrane technology has reached clinical stage and is currently the most widely used when gas exchange of native lungs fail completely. In translation research, three areas of enquiry have emerged, namely, bioengineered lungs, microfluidic technology and photocatalytic oxygenation of blood; these technologies are yet to reach clinical trials. The present photocatalytic oxygenation review has twofold purpose: the first, is to summarize the overall trajectory of lung assist device development, the second, is to describe the evolution of the concept of photocatalytic oxygenation as a potential method of increasing oxygen content of blood. The efforts so far have realized a proof of concept and a 6% increase in the oxygenation of blood with Titanium oxide and Indium tin oxide (TiO₂ + ITO) thin film photocatalyst. Photo Hall effect technique is employed to quantify the photocatalytic efficacy. This article reviews fundamental concepts as well as the progress made thus far and presents the challenges that need to be surmounted to realize the full potential of the technology at the bedside.

1. The need for oxygen as a bio-energetic fuel

The generation of oxygen by algal photosynthesis and the subsequent spike in oxygen levels of the atmosphere after the great oxygenation event (GOE) around 2–2.4 billion years ago helped establish oxygen as the most potent electron acceptor available. The significantly enhanced efficacy of aerobic over anaerobic of energy production set the stage for evolution to usher in the diversity and complexity of life on earth.

Central to the optimal functioning of the human body is the steady supply of oxygen to the tissues and its utilization by the cells for both ATP production (to do work) and heat production which in mammals and birds helps maintain their body temperature within a narrow range even in temperate and polar regions. Concomitant with oxygen utilization is the need to eliminate the carbon dioxide (formed as a result of cellular respiration) to the atmosphere to close the symbiotic cycle with plants.

2. Physiological aspects of gas exchange

In human, the heart and the lungs together form an integrated unit that has as its prime function the delivery of oxygen from the atmosphere to the cells and the return of carbon dioxide produced from cellular respiration to the atmosphere; this transportation is facilitated through the hemoglobin in the red blood cells of the blood. The proper functioning of the cardiopulmonary unit helps maintain oxygen and carbon dioxide levels that cells are exposed to within the physiological range. Exposure to cells to an excess or deficiency in either oxygen or carbon dioxide is associated with a variety of disease states.

The two basic aspects needed for optimal oxygen delivery to the blood are the gas exchange, the movement of oxygen into the blood stream and the reverse direction and ventilation the ability of carbon dioxide to move air into and out of the lungs from the atmosphere. Gas exchange is a function of the alveolar-capillary membrane in the lungs. Ventilation depends on the optimal and collaborative functioning of the central and peripheral nervous system, musculoskeletal system (diaphragm, muscles of chest,

abdomen neck and the ribcage) and the tracheo-bronchial tree. More details of the design factors that influence the vascular network on gas transfer mechanism are given in reference [1].

A multitude of diseases can affect the above systems to produce a loss of the gas exchange mechanism. Lack of supply of oxygen could result from disruption of normal ventilatory gas exchange or circulatory mechanisms and the degree of insult (mild symptoms of heart or lung failure to death) would depend on the speed and the depth of response of compensatory mechanisms. The lack of oxygen supply could be sudden (acute) or result from a steady loss of function over months or years (chronic) or the extrapolation of the former on the latter (acute on chronic).

3. An outline of some common diseases associated with poor oxygen delivery and its clinical impact

Acute respiratory failure with a sudden loss of gas exchange capability can occur in a wide range of diseases. It is a typical presentation of severe Acute Lung Injury (ALI), a clinical condition that results from a pathophysiological response in the lungs to a variety of acute diseases like trauma, pneumonias, bleeding, etc. It accounts for about 10% of Intensive Care Unit (ICU) admissions, however during epidemics such as swine flu [2] it can overwhelm critical care facilities. The mortality in severe ALI is around 40% [3].

Chronic respiratory diseases include Chronic obstructive pulmonary disease (COPD) from both smoking and non-smoking etiologies, air pollution related lung disease, interstitial lung diseases and its associated impaired gas exchange with subsequent failure of the right ventricle as it is called upon to work against an increasing pressure gradient accounts for significant mortality, morbidity and health related economic burden [4].

The cornerstone of treatment of ventilatory failure is positive pressure ventilation (PPV). The therapeutic value of PPV is limited in the face of a failing alveolar capillary interface in the lung. In addition the movement of air under pressure via the ventilator can cause trauma to the lungs which is in itself associated with an increased mortality and morbidity [5].

Current therapy is limited to ventilatory or gas exchange support in acute clinical situations. In chronic disease management involves medicines, aerosol nebulizers and physical rehab in the early part of the disease and oxygen therapy and lung transplantation for advanced stages.

4. Lung assist devices in clinical use

The evolution of lung assist devices from Schroder [6], von Frey and Gruber [7] to the present day has had a remarkable trajectory [8–13].

In short, it involved exposure of blood to oxygen or air in the gas phase (film oxygenator), or the introduction of oxygen into the blood phase (bubble oxygenator) or the physical separation of blood and gas with a barrier (membrane oxygenator) [14, 15].

The membrane oxygenators forms the basis for current oxygenators employed in the clinical use. A variety of materials from cellulose to synthetic polymers have been used but polymethylpentene (PMP) has emerged as material of choice in the present day oxygenators. Gas is passed through the lumen of hollow fibres and blood courses through the outside of these fibres facilitating gas exchange. The two basic configurations of the interface involve pores (0.3–0.7 μM) in about half the surface area of the fibre. This allows direct contact of the blood with gas phase initially but a membrane quickly develops as blood flows leading to a physical barrier. The second method has a physical polymer membrane that separates the blood from the gas phase at all times. The above innovations have increased the life of an oxygenator from hours in the case of bubble oxygenators to days to weeks in the present day Extra Corporeal Membrane Oxygenator (ECMO) devices [16].

5. Efficacy of current gas exchange support devices versus natural lungs

The current gas exchange devices are but a shadow of what the natural lungs can achieve (table 1). The basal oxygen consumption is around 250 mls min^{-1} which is well within the efficacy of current oxygenators.

The use of ventilators are associated with complications such as pneumonias, hemodynamic compromise and trauma to lung parenchyma. Gas exchange devices that provide extracorporeal life support are associated with bleeding, stroke, sepsis and disseminated intravascular coagulation [17].

Table 1. Comparison of dimensions and performance of oxygenators with natural lungs.

	Oxygenator	Lung
Surface area for gas exchange	1.3–2.5 m ²	160 m ²
Average distance of RBC from oxygen	>1 μ M	0.7 μ M
Peak exchange rate	450 ml min ⁻¹	2000 ml min ^{-1*}

* highest recorded in humans is 7000 ml min⁻¹

6. Areas of research in lung assist technology

There are three main areas of scientific enquiry can be identified in the lung assist technologies. The first involves bioengineering of lung tissue. This is accomplished by providing a scaffold on one side of which epithelial cells (the alveolar or air sac component) is cultured and on the other side the endothelial (capillary or blood vessel component) is cultured. The scaffolding could be entirely organic or synthetic or a hybrid. The process involves preserving the a cellular connective tissue scaffold of the lung (allogenic or xenogeneic in origin) after de-cellularisation and subsequent re-cellularisation with epithelial and endothelial cells on the scaffold [18, 19].

The second makes use of microfluidic technology and hopes to create a microenvironment that mimics the function of the alveolar capillary membrane—the so called ‘organ on a chip’ [20]. The potential advantages are the ability to create blood channels that use capillary action and laminar flow thereby reducing resistance to flow and the possible elimination or reduction in use of pumps. This may attenuate some of the complications in present day devices. The main hurdles in the above two methods are lack of clear understanding of the factors and mechanisms that ensure adequate embedding and proliferation of stem cells in the scaffold. In the case of the hybrid construct the hydrophobic nature of materials like silicone repels the cells and prevents cohesion. Bioengineered lungs while having demonstrated feasibility of cell survival have not yet adequately quantified gas exchange function [21].

The third area is the photocatalytic oxygenation. Photocatalysis is an established phenomenon: wherein, the light energy is used in the presence of a catalyst to split water into oxygen and hydrogen. Blood plasma contains 70% of water. The oxygen released from the photocatalysis of plasma is picked up by hemoglobin without any barrier (figure 1). This oxygenation technology has the potential, depending on the efficacy, to be used either as an assist or even complete replacement of the lungs. The efficacy of the process depends upon the material aspects of the photocatalyst and the charge transfer process across the catalyst—liquid interface [22, 23].

This is an emerging concept in the oxygenation of blood and this is the main topic of the present review. The proof of this concept has been worked out by Authors’ group [24–26] and the group of Dr. Richard Gilbert [27–30].

7. Basics of photocatalysis

The photocatalytic process consists of light (photons) of a suitable wavelength that generates an electron-hole pairs in the catalyst (a semiconducting material); the electrons are responsible for reduction of water to generate hydrogen and the holes initiate oxidation to generate oxygen. However, due to the difference in the energies in the oxidation and reduction mechanisms and the effective available electrons and the holes for these oxidation—reduction reactions, the general observation is that reduction process dominates over that of the oxidation. Thus, the requirement for oxidative process is to generate more number of holes with reasonably higher energy to overcome the semiconductor—liquid interface energy that participates in the photocatalytic process.

8. Oxidative photocatalysis

It is well known that the a photon (of energy higher than that of the band gap energy of the semiconductor) incident on the semiconductor, an electron—hole pair is generated; these electron—hole pairs travel to the surface of the catalyst and reacts with the liquid (electrolyte). The holes reacting with the liquid at the semiconductor—liquid interface produce OH^{*} and these OH^{*} with complex reactions produce oxygen molecules.

There is a vast literature on the oxidative photocatalysis. Among the several materials, the nano metal oxides and the plasmonic structures (having exceptional electronic, thermal and optical properties along with their biocompatibility) have attracted significant attention [31, 32]. Some of the recent nano metal

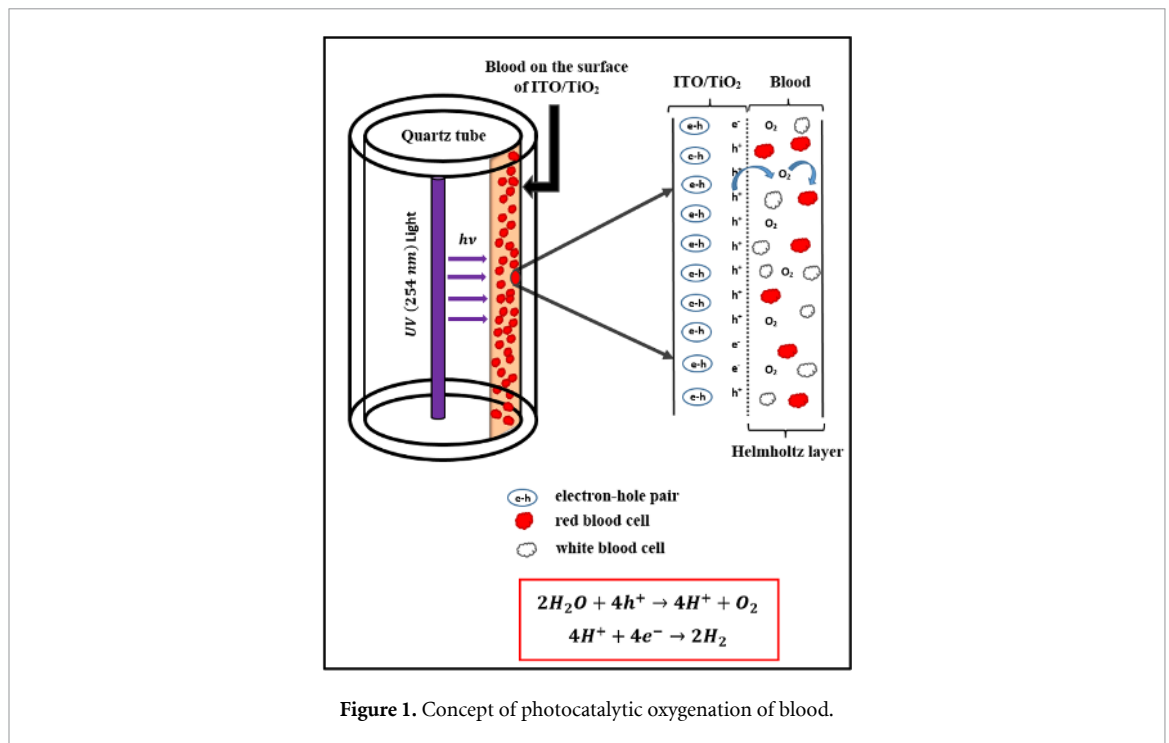


Figure 1. Concept of photocatalytic oxygenation of blood.

oxides like NiO nano sticks [33] and Co_3O_4 spinel nano particles show good promise for green chemistry applications [34].

The requirement of the photocatalysts for oxygenation of human blood are: (i) hemo compatibility, (ii) highly smooth surface of the catalyst (thin film) such that the blood constituents (red blood cells, white blood cells and platelets etc.,) do not stick onto the catalyst surface, (iii) the oxidative photocatalysis reaction should not swing the pH of blood below 7.35 and beyond 7.45 and (iv) the surface of the photocatalyst should not form any barrier coatings due to blood flow (for re-usability), (v) the oxygen produced in the photocatalytic process should not contain any reactive species and (vi) the photocatalytic efficacy should be reasonably high (band gap engineering).

Authors focused on ITO, TiO_2 and WO_3 thin films (prepared by reactive DC Magnetron sputtering technique) to work on the proof of concept of oxygenation of human blood, mainly because of their expertise and knowledge in these materials. These metal oxides are biocompatible [32, 35, 36].

All the prepared thin film photocatalysts have been characterized for their structural, morphological, electrical, and optical and photocatalytic properties. Rhodamine Dye has been used for oxidative photocatalysis experiments prior to the blood experiments.

9. Proof of concept of photocatalytic oxygenation of blood:

The possibility of using photocatalysis for blood oxygenation was initially established in static microfluidic [24, 25, 27], microfluidic [30] constructs and subsequently in a dynamic circuit [26]. The main challenge in conducting the oxygenation of blood by photocatalysis is the design of the photocatalytic reactor and a (clinical) circuit that does not allow any external oxygen. The details of the experimental protocols (for using blood) and the circuit for dynamic flow of blood are given in references [24] and [25]. The blood gas parameters (pH, Saturation Oxygen: SaO_2 etc) during the photocatalysis process are recorded by CDI Terumo blood gas monitor. The average (for over 25 experiments) percentage improvement in oxygen saturation (SaO_2) in dynamic experiments was shown to be around 6% employing ITO/ TiO_2 thin films [26]. The preliminary results (unpublished work from the Authors' laboratory) on ITO/ TiO_2 / WO_3 thin films show higher oxygen saturation (>9%), however, these results need more experiments for confirmation (WO_3 is well known material for water splitting).

10. Photocatalytic reactor

The photocatalytic (PC) reactor (figure 2) consists of a hollow quartz tube (length 250 mm and diameter of 25.2 mm and thickness of 1 mm and outer surface area of 175 cm^2). The photocatalyst thin films (ITO/ TiO_2 and ITO/ TiO_2 / WO_3) have been deposited on the outer surface of the quartz tube. Blood flows on the thin

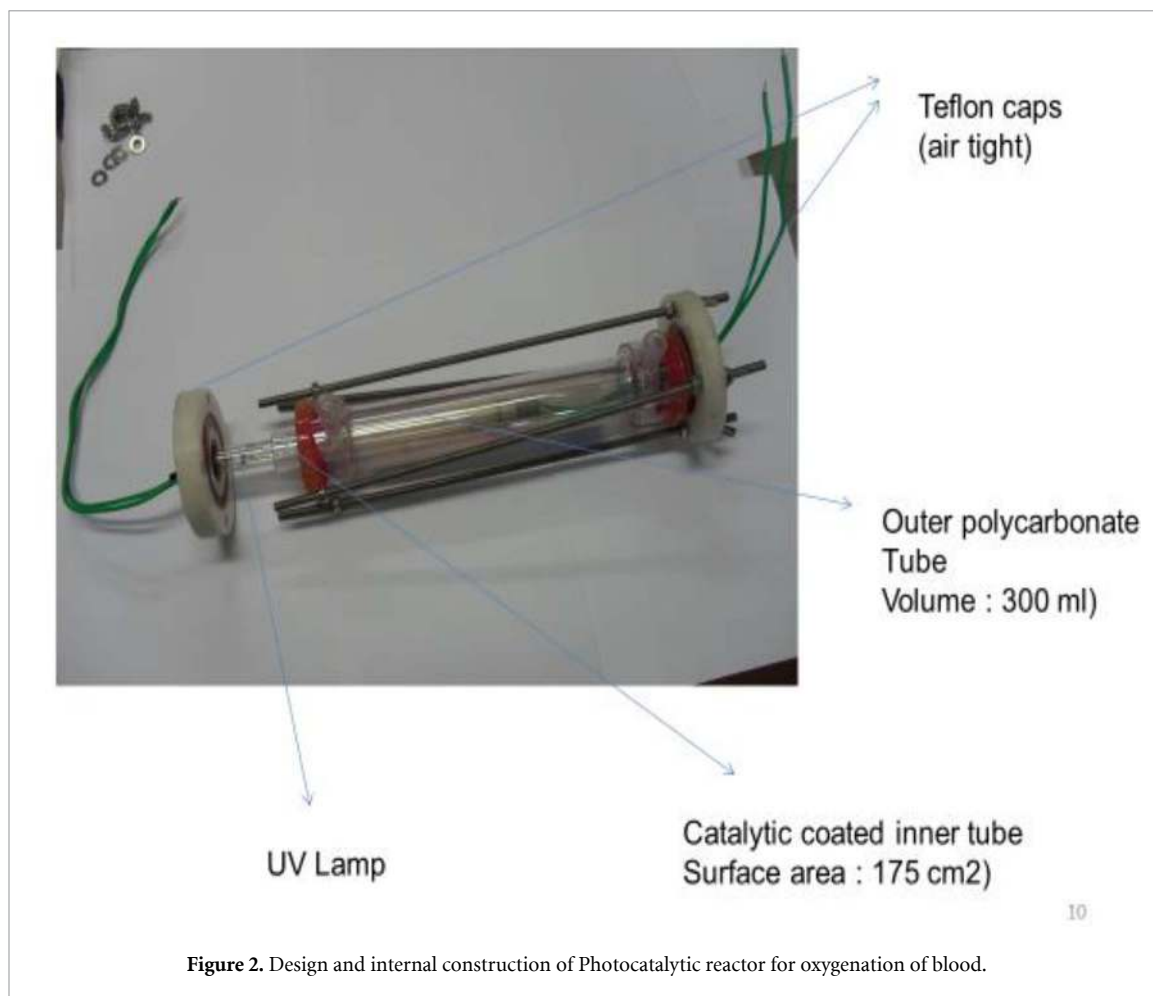


Figure 2. Design and internal construction of Photocatalytic reactor for oxygenation of blood.

films (the flow rate of the blood is controlled by a pump; these pumps are made by MC3 consultants, Michigan, USA).

This thin film coated quartz tube is enclosed in a polymer casing of a F5 renal dialyser (Fresenius Kabi, Germany) that has been modified by coring out the fibres and has been provided with air-tight inlet and outlet connectors for the blood to flow. The light source (UV lamp of wave-length 254 nm and 6 W; Sankyo Denki, Japan) inserted into the quartz tube such that the light from the source is transmitted through the inner surface of the quartz tube and passes through the photocatalytic thin film; this design eliminates the possibility of any direct exposure of blood to the UV light. Most of the light is absorbed in the photocatalyst and whatever remains passes through the blood. The volume of the reactor is 175 ml. The details of earlier experiments and of the photocatalyst are given in references [24, 25].

11. Brief details of the materials used

The thin films of ITO (of thickness $t = 450 \pm 5$ nm, optical band gap = 3.48 ± 0.02 eV and sheet resistance (R_s) ~ 120 ohms/square) and TiO_2 ($t = 50 \pm 5$ nm, optical band gap = 3.82 ± 0.02 eV) were deposited at room temperature ~ 300 K (by reactive DC magnetron sputtering) on the outer surface of a quartz tube. The TiO_2 thin films were annealed at 870 K for 60 min (in inert atmosphere) to obtain anatase structure. During this annealing, indium metal decorates TiO_2 surface. The distinctive features of these composite films lie in their oxygen deficiency and unique electron-hole pair separation ability.

12. Quantification/efficacy of the photocatalytic process

A preliminary understanding of the photocatalytic process may clarify the approach towards quantification. The light intensity is a measure of the number of photons and the wavelength specifies the energy of the photon. The basic process of photocatalysis consists of: (i) generation of electron-hole ($e-h$) pairs in the photocatalyst with the excitation wavelength (having an energy higher than the optical band gap of the photo-catalyst), (ii) transport of these $e-h$ pairs (after undergoing recombination and scattering in the

photocatalyst lattice) to the catalyst—liquid interface and (iii) a charge transfer process across the catalyst—liquid interface producing hydrogen and oxygen with several intermediate steps. Each of these steps need be quantified with precision. It may be noted that a quasi- equilibrium is attained when the generation rate equals with that of the recombination; at this quasi-equilibrium, the Fermi levels move towards the valence bands.

The actual photocatalytic process across the semiconductor—liquid interface is determined by the charge transfer process [23] which is highly complex and is beyond the scope of this review.

It is well known that the photo generated electron—hole pairs encounter several defects (recombination centres)/traps and only a fraction will reach the semiconductor surface; even in this fraction only those electrons and holes having enough kinetic energy participate in the charge transfer process across the photocatalyst—liquid interface to complete oxidative and reductive reactions producing oxygen and hydrogen respectively. It may be noted that the reactions are rate constant controlled (generally of the first order kinetics).

Traditional Chemists quantify the photocatalytic activity (for monochromatic wavelengths) by the Actinometry experiments [37]. The other approach of quantification (from Semiconductor physics point of view) for a thin film photocatalyst is to measure the (i) incident photon flux (at the wavelength the photocatalysis is being conducted) with a conventional flux meter, (ii) the number of photo-generated holes (minority carriers) reaching the semiconductor surface by conventional photo Hall effect experiment and (iii) the number of oxygen molecules produced in the liquid (by optical absorption measurements); generally any Dye (like Rhodamine) is used. Precautions to be exercised are: (i) to keep the intensity of the incident light constant, (ii) the photocatalyst thin film should be uniform across the entire surface and (iii) the pH of the liquid before starting the experiment should be kept constant.

For 100% efficient photon- material interactions, every photon produces an electron—hole pair. The efficacy of the photocatalyst materials being used is less than 5%. Design of new materials with higher quantum efficiency in electron—hole production and less number of defects may enhance the photocatalytic efficacy.

The Authors reported the quantification of the photocatalysis in blood experiments by measuring the photon flux and correlating the number of photons to the number of oxygen molecules produced [26]. The incident wavelength is 254 nm. The measured average photon flux (Thor labs PM100A, Dachau, Germany) on a bare quartz tube surface is: 19.08×10^{15} photons $\text{cm}^{-2} \text{sec}^{-1}$; the flux measured on the ITO/TiO₂ coated tube surface is: 9.095×10^{15} photons $\text{cm}^{-2} \text{sec}^{-1}$. Thus $9.98 (\sim 10) \times 10^{15}$ photons $\text{cm}^{-2} \text{sec}^{-1}$ are absorbed by the photocatalyst. The number of holes generated in the photocatalyst is measured with photo Hall effect experiment (details in appendix A). Extreme caution is to be exercised while measuring the hole density, the minority carriers. One can calculate the efficacy by measuring the number of dye (Rhodamine) molecules oxidized.

Photo Hall effect (Lakeshore HMS 7604 with Quantitative Mobility Spectrum Analyser (QMSA) software) measurements (with 254 nm light) have shown that in six hours, the hole concentration reached a steady state is $\sim 10^{17}$ carriers cm^{-2} and the Hole mobility is $\sim 1 \text{ cm}^2 \text{V}^{-1} \text{s}^{-1}$ (unpublished data).

Summary on quantification by Photo Hall effect with Rhodamine Red dye oxidation (appendix A):

Efficacy of photocatalytic process: $0.442 \times 10^{-2}\%$.

The quantum efficiency of the photocatalyst: 0.056%.

The efficacy can be improved with nano metal oxides that produce large number of holes with sufficient energy to participate in the charge exchange process to produce oxygen.

13. Oxygen species produced in the photocatalytic process

Photocatalytic process produces several oxidative intermediates (like the hydroxyl radicals and singlet oxygen, etc.), produced during the photocatalytic activity forming hydrogen peroxide, superoxide, and hydroxyl radicals.

Generally, the process of photo-generated electron-hole pairs in the presence of the catalyst (TiO₂–ITO) may be represented by the following intermediate steps [26, 30, 38]



The photo-generated electron (e^-)—hole (h^+) pairs reach the catalyst surface-liquid interface; at this interface, two prominent reaction routes are possible: the hole can interact with surface bound molecules

(water or dye); electrons were captured by oxygen molecules adsorbed on the film surface to give superoxide radicals [26, 30, 39].



The study conducted by the Authors with isopropanol and benzoquinone clearly indicated the presence of the formation of superoxide and the prepared TiO₂/Ti-ITO catalyst can *in situ* generate oxygen molecules [39]. The conventional method to detect any reactive oxygen species is Electron Paramagnetic Resonance (EPR) experiment. What is needed in the oxygenation of blood is oxygen molecules only.

14. Reusability of the photocatalyst

TiO₂-ITO thin film photocatalysts have been studied for their re-usability. Photocatalytic performance with twelve consecutive cycles for Rhodamine Red and three cycles of blood clearly indicate that the catalyst is reusable without much loss of performance. It may be noted that the repeatability cycles were performed after a resting time of 8–10 h between each cycle, which may aid the equilibration of electron hole-reset to bring the material to its original condition (appendix A). Upon repeated usage of 60–80 times, there is a slight decrease in the catalytic efficiency (5%–8% decrease), which could be due to surface damage probably due to scratches or mechanical abrasions during handling and cleaning. Overall, the prepared catalytic films have been found to be special class of materials, which need further investigation for a better exploitation in various applied fields.

15. Challenges and opportunities in the photocatalytic oxygenation of blood

Having proven the concept of oxygenation of blood by photocatalytic process, one desires to enhance the efficacy of the process so that it can be used as lung assist device.

The foremost challenge is to enhance the efficacy of the photocatalytic oxygenation process to reach 250 ml min⁻¹: the basal requirement at rest of an average adult. The fond hope is that with new materials and material design methodologies and new efficient white light sources in photocatalysis, the requirement can be met with.

Caution must be exercised that the photocatalysis process should not produce Reactive oxygen species (ROS) as final products; there is evidence that these reactive species could be harmful [26, 30]. The production, quantity and the nature of reactive oxygen species produced in photocatalytic process needs more detailed study.

The harmful effects of UV wavelength in causing DNA damage have been well described, more recently with the emergence of multi-drug resistant bacteria the use of UV light as potential therapy is being re-evaluated [40, 41]. The intensity and dose will require further study and refinement and the possibility of visible light photocatalysis as an alternative must be investigated.

As the incidence of lung diseases increases with its attendant mortality and morbidity, it becomes imperative to seek solutions that are safe, durable and affordable. The question as to which of the technologies will emerge as a forerunner or indeed if they will converge and result in a composite device is one that only further research and time can answer.

Acknowledgments

The Authors gratefully acknowledge the support of M/s HCL Technologies, India and the Department of Biotechnology (DBT), Government of India for financial support. The efforts of all the project staff associated with the work is gratefully acknowledged.

Appendix A

Photo-conductivity and photo Hall effect [42, 43] can be used to quantify the photocatalytic efficacy. The conventional Hall effect experiment measures the concentration and mobility of majority charge carriers in a semiconductor [44]. When a light of higher energy than the band gap of the semiconductor is incident, electron-hole (e)-(h) pairs are generated; the minority carrier concentration increases significantly

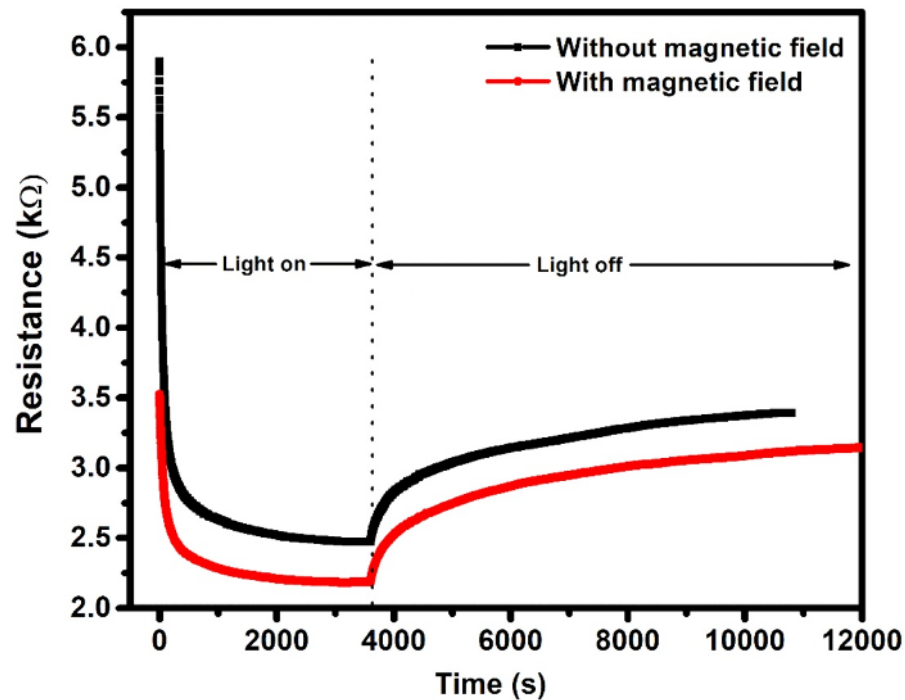


Figure A1. Electrical Resistance measurement (using conventional measurement system) performed on the entire ITO/TiO₂ photocatalyst tube of area 175 cm². The resistance is measured when UV 254 nm light is on and off.

depending upon the incident light intensity, band gap and absorption coefficient of the semiconductor. When majority and minority carriers differ by one or two orders of magnitude, models such as Quantitative Mobility Spectrum Analyser: QMSA) are to be used in estimating the minority carrier concentration and mobility [45].

The photoconductivity experiment on ITO/TiO₂ photocatalyst is conducted (using source meter Keithley SMU 2400) with a conventional set up with an accuracy of 0.1 ohm. As soon as the UV light of 254 nm wavelength is incident on the photocatalyst, the resistivity shows an exponential decay (figure A1) and reaches a constant values after 2000 s. When the illumination is turned off (at 3600 s as shown in figure A1), the resistivity increases slowly. The same experiment is conducted in a magnetic field of 4000 Gauss (red curve in figure A1), the resistance decreases significantly.

The photoconductivity experiment is also conducted with the automated Hall measurement system (without the magnetic field); the results are similar and are presented in figure A2.

The difference between the two experiments (figures A1 and A2) is that the conventional photoconductivity is performed on the entire area of the photocatalyst (175 cm²) and the second experiment (HMS 7406) is done on the sample of area 1 cm × 1 cm.

After about 2000 s, the resistivity shows a fairly constant value. When the illumination is switched off, the resistivity (i) does not come back to the original 'dark' resistivity value and (ii) there are significant variations in the resistivity with time. It takes almost 72 h for the photocatalyst to return to its original 'dark' value. These observations are repeatable not only in magnitude but also in behaviour.

The aim of conducting the electrical resistivity measurements is (i) to estimate the relaxation/recoument time of the photocatalyst and (ii) to ascertain the behaviour of the material is not dependent on the size in the measurements. More detailed experiments are needed to understand the long relaxation time of the photocatalyst: ITO/TiO₂

A.1. Hall effect experiment:

The automated Hall effect experiments (HMS 7406) have been conducted on the photocatalysts described in section 11 [46]. 1 cm × 1 cm area of the photocatalyst is isolated on the photocatalytic tube to obtain the van der Paw configuration. Indium metal is soldered at all the four corners for ohmic contacts. The quartz tube is placed between the magnetic poles. The UV lamp (254 nm wavelength, Sankyo Denki, Japan, 6 W) is inserted into the quartz tube such that the photocatalyst is illuminated from the rear side (this is how the experiments with blood have been conducted). The lamp characteristics have not been changed even after

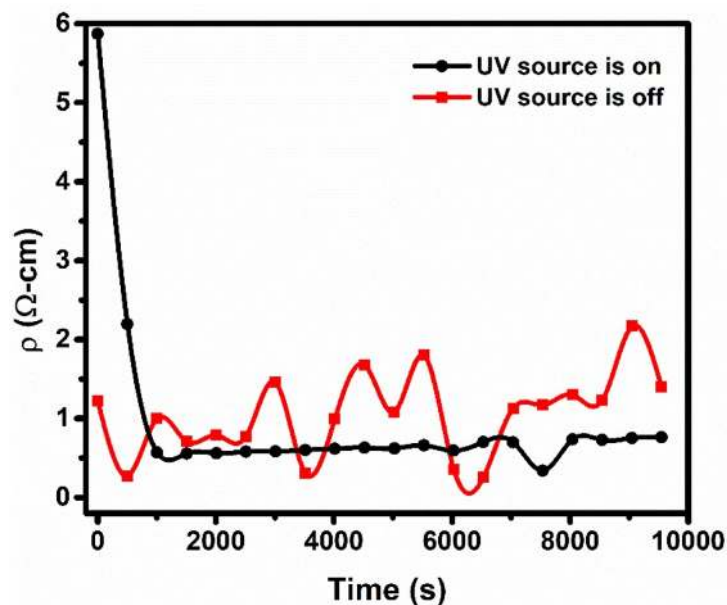


Figure A2. Resistivity measurement (using HMS 7406) performed on 1 cm × 1 cm ITO/TiO₂ photocatalyst coated on quartz tube. The resistivity is measured when UV 254 nm light is on (black curve) and off (red curve).

the magnetic field is applied. The fluctuations shown in the resistivity and the Hall data are repeatable over several runs; hence they are not due to the Instrument but the property of the photocatalyst.

The details of the photon flux measurements are given in section 12. The Hall effect results are analysed with Quantitative Mobility Spectrum Analyser (QMSA).

The Hall measurement system performs the ohmic contact check before any measurement. After the 'dark' measurements are successful, the illumination (254 nm wavelength) is switched on. The Hall effect experiment in the 'dark' condition, shows a n-type carriers (of concentration $4.3 \times 10^{16} \text{ cm}^{-3}$) for ITO/TiO₂; the Hall mobility in 'dark' for these electrons is $26.2 \text{ cm}^2 \text{ V}^{-1} \text{ s}^{-1}$. With illumination, one expects an increase in the carrier concentration and the Hall mobility. However, the results show that the electron concentration initially decreases and electron Hall mobility increases; one important observation is that the holes do appear in the measurement (figure A3). With illumination, the measurement gives a mixed n and p type carrier density (figure A3(a)); the corresponding Hall mobility of the respective carriers is given in figure A3(b)).

As a function of time, both electron and hole concentrations and mobilities are almost the same order and the type of conductivity fluctuate (the measurement being automatic, this is true representation of the observation). This observation reminds the limitation of the conventional Hall effect measurement when the majority and minority carrier concentrations differ by a few orders [47]. We should invoke the detailed analyses proposed by QMSA [45].

A.2. Photocatalysis experiments with Rhodamine Red Dye

For the quantification of efficacy, the photocatalytic results of ITO/TiO₂ catalyst with 254 nm illumination performed with 0.1 Molar freshly prepared Rhodamine B dye (of pH 7.35) is presented in the figure A4. The photocatalytic experiment is also conducted in the presence of magnetic field (since Hall effect involves magnetic fields). The photocatalytic activity initially decreases with magnetic field, but with increasing time, the activity shows a slight increase.

A.3. Inference

What is known: The ITO/TiO₂ is an n type semiconductor (as seen by the Hall experiments without illumination). As soon as the 254 nm wavelength light is incident on the photocatalyst, electron—hole (e-h) pairs are generated. The photo-generated electrons are much less in number; hence the electron concentration (the majority carriers) in the semiconductor is practically unaltered. These photo-generated carriers (e-h pairs) are responsible for the (exponential) decrease in the resistivity of the semiconductor as seen from figures A1 and A2. The photo-generated carriers experience either recombination or/and trapping at the defect levels (includes surface defects). When the photo-generation rate equals with the recombination

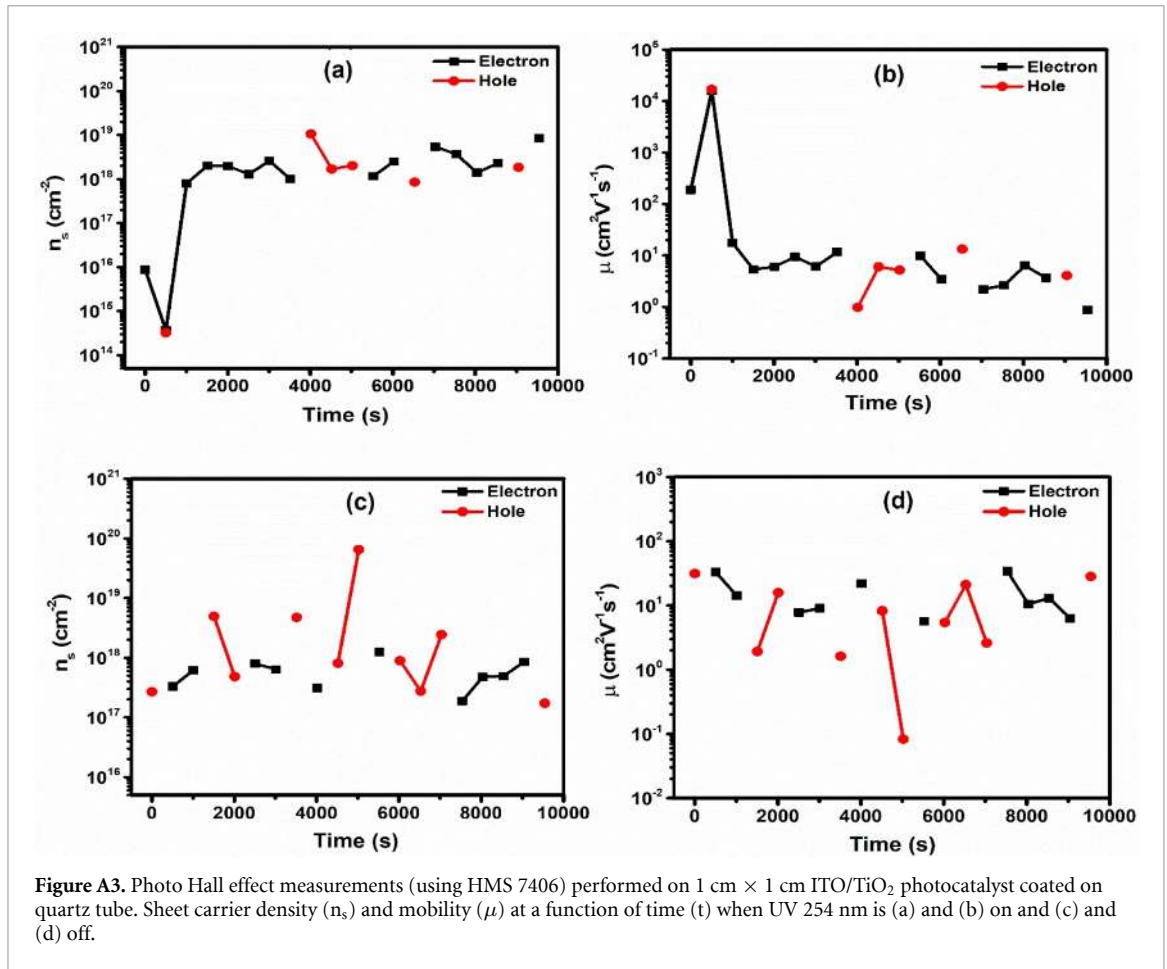


Figure A3. Photo Hall effect measurements (using HMS 7406) performed on 1 cm × 1 cm ITO/TiO₂ photocatalyst coated on quartz tube. Sheet carrier density (n_s) and mobility (μ) at a function of time (t) when UV 254 nm is (a) and (b) on and (c) and (d) off.

Table A1. Parameters extracted from the photocatalysis measurements (figure A4) performed without magnetic field.

t (min)	A	ΔA	$C_t (\times 10^{-5})$	$n_1 (\times 10^{18})$	$n_{180} (\times 10^{18})$	$n_0 (\times 10^{17})$	$n_0/a (\times 10^{15})$	$n (\times 10^{13})$	$\ln(C_0/C_t)$
BRE	2.01	0	1.56	9.43	1.69	0	0	0	0.28
30	1.98	1.49	1.54	9.29	1.67	0.24	0.14	0.47	0.30
60	1.89	5.97	1.47	8.87	1.59	1.00	0.57	0.96	0.34
90	1.78	11.44	1.38	8.35	1.50	1.93	1.10	1.23	0.40
120	1.69	15.92	1.31	7.93	1.42	2.69	1.54	1.28	0.46
180	1.52	24.37	1.18	7.13	1.28	4.13	2.36	1.31	0.56
240	1.39	30.84	1.08	6.52	1.17	5.23	2.99	1.24	0.65
300	1.29	35.82	1.00	6.05	1.09	6.07	3.47	1.15	0.73
Total: 7.64									

t = time, A = absorbance, ΔA = change in absorbance, C_t = concentration at time t, n_1 = number of oxidized molecules per litre, n_{180} = number of molecules oxidized per 180 ml, n_0 = number of molecules oxidized, a = area, n = number of molecules oxidized per unit area per unit time.

rate (along with the trapping of the carriers), a quasi-static equilibrium is established. At quasi-static equilibrium, the semiconductor reaches a constant resistivity. In ITO/TiO₂, at the quasi-static equilibrium, the quasi Fermi level (under illumination) moves towards the valence band. At the semiconductor—liquid interface, because of the Fermi level movement, the band bending is anticipated to bend downwards resulting in the hole transfer across the interface facilitating oxidative process in the Rhodamine B dye. The charge transfer (both electrons and the holes) across the interface and the intermediate reactions are quite complex.

It is well known that when the illumination is switched off, it is anticipated that the semiconductor returns to its original equilibrium to attain ‘dark’ resistivity in a time known as ‘relaxation time’. Generally, the relaxation time spans in milli seconds or seconds depending upon the semiconductor. However, the observation in the present study is that the relaxation time is of the order of several tens of hours (72 h). Several attempts: shorting the two ohmic contacts, immersion of the semiconductor in conducting water (at room temperature), reversing the voltage terminals, did not influence the long relaxation time of this

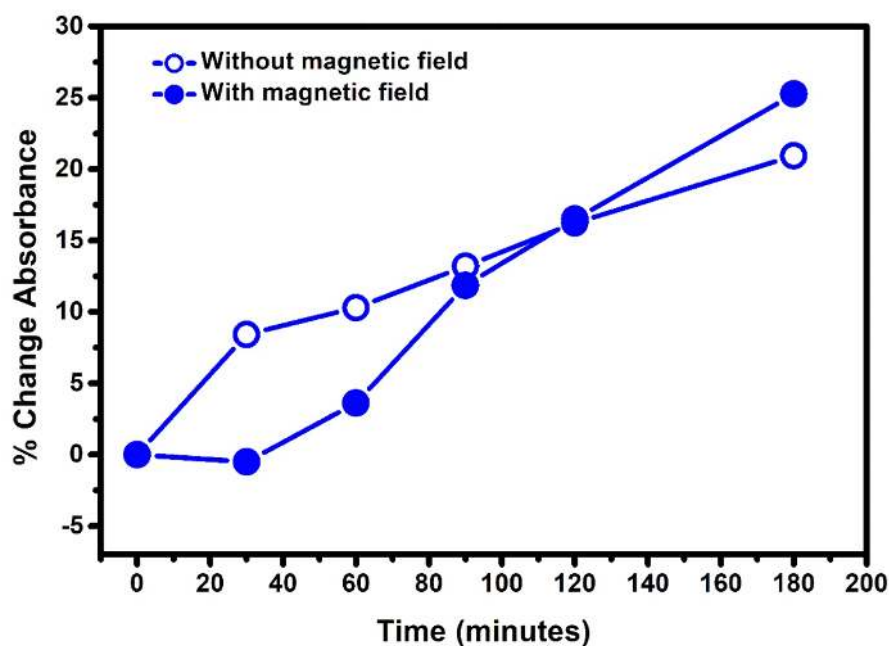


Figure A4. Photocatalysis measurements performed on ITO/TiO₂ photocatalyst coated on quartz tube. The measurement is carried out with magnetic field (filled circles) and without magnetic field (open circles) respectively.

ITO/TiO₂ semiconductor. This observation points out that the photo-generated charge if trapped in a deep defect level, such relaxation is possible; however, more detailed study is required for a deeper understanding.

Quantitative Mobility Spectrum Analyzer (QMSA) proposes to fit a model with concentrations and mobility of the two types of carriers. The underlying principle being that high magnetic fields induce a non-linearity in the mobility values, particularly of the holes because of their heavy masses (heavy holes and light holes). When the QMSA model is applied to the data obtained in the present study, the results are very interesting (figure A3). The holes appear intermittently and show spikes in both the carrier density and Hall mobility. If this were true, one should also observe the oxidation kinetics of the liquid (figure A4). Under such conditions, the pseudo first order reaction kinetics may not be valid. One very important observation the Authors noticed very repeatedly is that when human blood is photocatalyzed, the oxidation is not linear: it shows intermittent steps.

A.4. Quantification summary

The incident photon flux over the entire 175 cm² area in 300 min (at 254 nm):

$$19.03 \times 10^{15} \times 175 \text{ cm}^2 \times (300 \times 60 \text{ s}) = 5.99 \times 10^{22} \text{ photons}$$

Number of Photons absorbed by the photocatalyst: $9.98 \times 10^{15} \times 175 \text{ cm}^2 \times (300 \times 60 \text{ s}) = 3.1 \times 10^{22}$ Photons

$$\text{Number of holes produced in the photocatalyst: } 10^{17} \times 175 \text{ cm}^2 = 1.75 \times 10^{19}$$

$$\text{Number of Rhodamine Red molecules oxidized in 300 min} = 7.64 \times 10^{13} \times 300 \times 60 = 1.37 \times 10^{18}$$

$$\text{Efficacy of photocatalytic process: } [(1.37 \times 10^{18}) / (3.1 \times 10^{22})] = 0.442 \times 10^{-2}\%$$

$$\text{The quantum efficiency of the photocatalyst} = [(1.75 \times 10^{19}) / (3.1 \times 10^{22})] = 0.056\%$$

It is a little surprising to see that 16.13×10^{18} holes did not participate in the oxidation process.

Since the mobility of these holes is rather low (1 cm²/v/s), some of them might have been lost in the recombination process and some of the holes might not have enough energy for the oxidation process at the semiconductor—liquid interface.

The Photo Hall effect is a method to quantify the Photocatalytic efficacy of Thin film Photocatalysts.

ORCID iD

A Subrahmanyam  <https://orcid.org/0000-0001-5532-369X>

References

- [1] Bassett E K, Hoganson D M and Lo J H Penson E J N and Vacanti J P 2011 Influence of vascular network design on gas transfer in lung assist device technology *Asaio J.* **57** 533–8
- [2] Hendrickson C M and Matthay M A 2013 Viral pathogens and acute lung injury: investigations inspired by the SARS epidemic and the 2009 H1N1 influenza pandemic *Seminars in Respiratory and Critical Care Medicine* (Thieme Medical Publishers) pp 475–86
- [3] Thompson B T, Chambers R C and Liu K D 2017 Acute respiratory distress syndrome *N. Engl. J. Med.* **377** 562–72
- [4] Forum of International Respiratory Societies 2017 The Global Impact of Respiratory Disease Second ed (Sheffield: European Respiratory Society) pp 1–43
- [5] Thompson B T, Bernard G R and Network A R D S 2011 (NHLBI) studies: successes and challenges in ARDS clinical research *Crit. Care Clin.* **27** 459–68
- [6] Schroeder W V 1882 über die Bildungsstätte des Harnstoffs *Archiv. Für. Experimentelle. Pathologie. Und. Pharmakologie.* **15** 364–402
- [7] Frey von M and von Gruber M 1885 Untersuchungen über den Stoffwechsel isolierter Organe: ein Respirations-Apparat für isolierte Organe *Virchow's Arch. Physiol.* **9** 519–32
- [8] Hammell C, Forrest M and Barrett P 2008 Clinical experience with a pumpless extracorporeal lung assist device *Anaesthesia* **63** 1241–4
- [9] Wermelt J Z, Honjo O, Kilic A, van Arsdell G, Gruenwald C and Humpl T 2008 Use of a pulsatile ventricular assist device (Berlin Heart EXCOR) and an interventional lung assist device (Novalung) in an animal model *Asaio J.* **54** 498–503
- [10] Wu Z J, Taskin M E, Zhang T, Fraser K H and Griffith B P 2012 Computational model-based design of a wearable artificial pump-lung for cardiopulmonary/respiratory support *Artif. Organs* **36** 387–99
- [11] Ertan Taskin M et al 2016 Design optimization of a wearable artificial pump-lung device with computational modeling *J. Med. Device* **6** 031009
- [12] Zhang T, Wei X, Bianchi G, Wong P M, Biancucci B, Griffith B P and Wu Z J 2012 A novel wearable pump-lung device: in vitro and acute in vivo study *J. Heart Lung Transplant.* **31** 101–5
- [13] Maul T M, Nelson J S and Wearden P D 2018 Paracorporeal lung devices: thinking outside the box *Frontiers in Pediatrics* **6** 243
- [14] Hamid I A, Hariharan A S and Shankar N R R 2010 The advent of ECMO and pumpless extracorporeal lung assist in ARDS—a review *Indian J. Thoracic Cardiovascular Surg.* **26** 280–8
- [15] Faria M and De Pinho M N 2015 Extracorporeal blood oxygenation devices, membranes for *Encyclopedia of Membranes Berlin Drioli, Enrico, Giorno, Lidietta* (Eds.) (Heidelberg: Springer Berlin Heidelberg) pp 1–19
- [16] Shekar K, Mullany D V, Thomson B, Ziegenfuss M, Platts D G and Fraser J F 2014 Extracorporeal life support devices and strategies for management of acute cardiorespiratory failure in adult patients: a comprehensive review *Crit. Care* **18** 219
- [17] Knudson K A, Gustafson C M, Sadler L S, Whittemore R, Redeker N S, Andrews L K, Mangi A and Funk M 2019 Long-term health-related quality of life of adult patients treated with extracorporeal membrane oxygenation (ECMO): an integrative review *Heart Lung* **48** 538–52
- [18] Lemon G et al 2014 The development of the bioartificial lung *British Medical Bulletin* **110** 35–45
- [19] Guenthart B A, O'Neill J D, Kim J, Fung K, Vunjak-Novakovic G and Bacchetta M 2019 Cell replacement in human lung bioengineering *J. Heart Lung Transplant.* **38** 215–24
- [20] Bleilevens C, Lölsberg J, Cinar A, Knoblen M, Grottko O, Rossaint R and Wessling M 2018 Microfluidic cell sorting: towards improved biocompatibility of extracorporeal lung assist devices *Sci. Rep.* **8** 1–9
- [21] Nichols J E et al 2018 Production and transplantation of bioengineered lung into a large-animal model *Science Translational Medicine* vol 10 pp 14–19 eaa03926
- [22] Fujishima A and Honda K 1972 Electrochemical photolysis of water at a semiconductor electrode *nature* **238** 37–38
- [23] Rajeshwar K 2007 Fundamentals of semiconductor electrochemistry and photoelectrochemistry *Encyclopedia Electrochem.* **6** 1–53
- [24] Subrahmanyam A, Ramesh T P and Ramakrishnan N 2007 Oxygenation of human blood using photocatalytic reaction *Asaio J.* **53** 434–7
- [25] Subrahmanyam A, Arokiadoss T and Ramesh T P 2007 Studies on the oxygenation of human blood by photocatalytic action *Artif. Organs* **31** 819–25
- [26] Subrahmanyam A, Thangaraj P R, Kanuru C, Jayakumar A and Gopal J 2014 Quantification of photocatalytic oxygenation of human blood *Med. Eng. Phys.* **36** 530–3
- [27] Dasse K A, Monzyk B F, Burckle E C, Busch J R and Gilbert R J 2003 Development of a photolytic artificial lung: preliminary concept validation *Asaio J.* **49** 556–63
- [28] Monzyk B F, Burckle E C, Carleton L M, Busch J, Dasse K A, Martin P M and Gilbert R J 2006 Photolytically driven generation of dissolved oxygen and increased oxyhemoglobin in whole blood *Asaio J.* **52** 456–66
- [29] Gilbert R J, Carleton L M, Dasse K A, Martin P M, Williford R E and Monzyk B F 2007 Photocatalytic generation of dissolved oxygen and oxyhemoglobin in whole blood based on the indirect interaction of ultraviolet light with a semiconducting titanium dioxide thin film *J. Phys. D: Appl. Phys.* **102** 73512
- [30] Rasponi M, Ullah T, Gilbert R J, Fiore G B and Thorsen T A 2011 Realization and efficiency evaluation of a micro-photocatalytic cell prototype for real-time blood oxygenation *Med. Eng. Phys.* **33** 887–92
- [31] Kudo A 2003 Photocatalyst materials for water splitting *Catal. Surv. Asia* **7** 31–38
- [32] Huang H, Fan X, Hao Q, Du D, Luo X and Qiu T 2016 Exploring indium tin oxide capped titanium dioxide nanolace arrays for plasmonic photocatalysis *RSC Adv.* **6** 12611–5
- [33] Rajan P I, Vijaya J J, Jesudoss S K, Kaviyarasu K, Kennedy L J, Jothiramalingam R, Al-Lohedan H A and Vaali-Mohammed M-A 2017 Green-fuel-mediated synthesis of self-assembled NiO nano-sticks for dual applications—photocatalytic activity on Rose Bengal dye and antimicrobial action on bacterial strains *Mater. Res. Express* **4** 85030
- [34] Jesudoss S K, Vijaya J J, Rajan P I, Kaviyarasu K, Sivachidambaram M, John Kennedy L, Al-Lohedan H A, Jothiramalingam R and Munusamy M A 2017 High performance multifunctional green Co₃O₄ spinel nanoparticles: photodegradation of textile dye effluents, catalytic hydrogenation of nitro-aromatics and antibacterial potential *Photochem. Photobiol. Sci.* **16** 766–78
- [35] Harnett E M, Alderman J and Wood T 2007 The surface energy of various biomaterials coated with adhesion molecules used in cell culture *Colloids Surf. B* **55** 90–97
- [36] López-Huerta F, Cervantes B, González O, Hernández-Torres J, García-González L, Vega R, Herrera-May A and Soto E 2014 Biocompatibility and surface properties of TiO₂ thin films deposited by DC magnetron sputtering *Materials* **7** 4105–17
- [37] Asenath-Smith E, Ambrogio E K, Moores L C, Newman S D and Brame J A 2019 Leveraging chemical actinometry and optical radiometry to reduce uncertainty in photochemical research *J. Photochem. Photobiol. A* **372** 279–87

- [38] Long T C, Saleh N, Tilton R D, Lowry G V and Veronesi B 2006 Titanium dioxide (P25) produces reactive oxygen species in immortalized brain microglia (BV2): implications for nanoparticle neurotoxicity *Environ. Sci. Technol.* **40** 4346–52
- [39] Subrahmanyam A, Rajakumar A, Rakibuddin M, Paul Ramesh T, Raveendra Kiran M, Shankari D and Chandrasekhar K 2014 Efficacy of titanium doped-indium tin oxide (Ti/TiO₂-ITO) films in rapid oxygen generation under photocatalysis and their suitability for bio-medical application *Phys. Chem. Chem. Phys.* **16** 24790–9
- [40] Hamblin M R 2017 Ultraviolet irradiation of blood: “the cure that time forgot”? *Ultraviolet Light in Human Health, Diseases and Environment* (Berlin: Springer) pp 295–309
- [41] Nichols C E, Shepherd D L, Hathaway Q A, Durr A J, Thapa D, Abukabda A, Yi J, Nurkiewicz T R and Hollander J M 2018 Reactive oxygen species damage drives cardiac and mitochondrial dysfunction following acute nano-titanium dioxide inhalation exposure *Nanotoxicology* **12** 32–48
- [42] Bube R H, MacDonald H E, Blanc J 1961 Photo-hall effects in photoconductors *Journal of physics and chemistry of solids* **22** 173–180
- [43] Bube R H 1978 *Photoconductivity of solids* (Malabar, FL: Kreiger)
- [44] Putley E H 1960 *The Hall effect and related phenomena* (Butterworth)
- [45] Du G, Lindemuth J R, Dodrill B C *et al* 2002 Characterizing multi-carrier devices with quantitative mobility spectrum analysis and variable field Hall measurements *Japanese journal of applied physics* **41** 1055
- [46] Subrahmanyam A, Rajakumar A, Rakibuddin M *et al* 2014 Efficacy of titanium doped-indium tin oxide (Ti/TiO₂-ITO) films in rapid oxygen generation under photocatalysis and their suitability for bio-medical application *Physical Chemistry Chemical Physics* **16** 24 790–9
- [47] McKelvey J P 1966 *Solid state and semiconductor physics* (New York: Harper & Row)